Activated carbon supported Fe, Ni, and Ni-Fe bimetallic catalysts for CO_x-free H_2 production by microwave methane pyrolysis

Candice Ellison[1,2], Julia Lauterbach[1,3,4], Mark W. Smith[1,*]

[1]National Energy Technology Laboratory, Morgantown, WV, USA

[2]USDA-ARS Eastern Regional Research Center, Wyndmoor, PA, USA

[3]Oak Ridge National Laboratory, Oak Ridge, TN, USA

[4]Wake Forest University, Winston-Salem, NC, USA

The goal of this study was to test the effect of metal-impregnated carbon-based catalysts on the conversion of methane to hydrogen gas and solid carbon using microwave reactor technology. Monometallic and bimetallic catalysts on activated carbon supports (Ni/AC, Fe/AC, Ni-Fe/AC) are compared during methane pyrolysis testing. Catalytic methane pyrolysis was carried out in a microwave reactor at reaction temperatures of 600 °C and 800 °C. For comparison, one of the catalysts (Ni-Fe/AC) was tested in a conventionally heated reactor at 800 °C. The prepared catalysts were characterized by X-ray diffraction (XRD), while post-reaction catalysts were characterized by XRD and SEM. During reaction testing, the monometallic Ni/AC catalyst exhibited the best catalytic activity (CH_4 conversion: 46.0 and H_2 yield: 46.9%) when reacted in the microwave reactor, however, it suffered from rapid deactivation from carbon deposition (carbon yield: 0.39 g C/g catalyst). The bimetallic Ni-Fe/AC catalyst was slightly less active (CH_4 conversion: 36.9 and H_2 yield: 40.5%) but it was more resistant to carbon formation (carbon yield: 0.27 g C/g catalyst) suggesting it may have greater long-term stability. The Ni-Fe/AC catalyst was also the most energy efficient as it required the least microwave power to maintain the 800 °C reaction temperature compared to the other catalysts tested. Methane conversion of the bimetallic Ni-Fe/AC at 800 °C under microwave irradiation was three times the conversion under conventional heating at the same reaction temperature. This work demonstrates the use of microwave-specific catalysts for catalytic methane pyrolysis in a microwave reactor, and can be used as a foundation for further methane pyrolysis process and catalyst optimization for CO_x-free H_2 production.

Keywords: Methane pyrolysis, heterogeneous catalysis, microwave, bimetallic catalyst

*Corresponding author: mark.smith@netl.doe.gov, 3610 Collins Ferry Rd., Morgantown,WV 26507

1. Introduction

The development of low- and zero- CO_2 emission fuels has been a focus in the renewable energy field for years [1]. It has recently come to the forefront of energy research in the United States with the implementation of the Bipartisan Infrastructure Law, which includes more than $62 billion for the U.S. Department of Energy (DOE) to deliver a more equitable clean energy future for the American people. The United States has made it a mission to reduce the country's greenhouse gas emissions by 65 percent by 2030 and achieve net-zero emissions by 2050 [2].

With this goal in mind, many researchers have begun to focus on the promising clean energy sector of hydrogen. This clean fuel produces only water when combusted in a hydrogen internal combustion engine or when consumed in a fuel cell. Hydrogen is currently being produced from a variety of different sectors, such as natural gas, nuclear power, biomass, and renewable power like solar and wind via electrochemical water splitting [3]. Methane, the main component of natural gas, has the highest hydrogen content out of all hydrocarbons [3] and is, therefore, very valuable as a hydrogen feedstock for the chemical industry. Methane is also abundantly produced as a byproduct of the agriculture industry and is the main component of renewable gas (biogas) produced by organic matter fermentation. Hydrogen recovery from renewable sources of methane (biomethane) offers a pathway for low-carbon hydrogen production.

Several different processes have been developed to produce hydrogen from methane. Steam reforming of methane is currently the most commercially used and cost-effective method for hydrogen production, and it produces over 50% of the world's hydrogen [4]. Steam reforming involves heating methane and steam to temperatures up to 1,200 °C, typically over a nickel-

based catalyst. This strongly endothermic reaction produces CO and H_2 via the following reaction:

$$CH_4 + H_2O \rightarrow CO + 3H_2 \quad (1)$$

CO can be reacted with more steam, typically over an iron-based catalyst, to obtain more hydrogen via the water-gas shift reaction:

$$CO + H_2O \rightarrow CO_2 + H_2 \quad (2)$$

While steam reforming is a mature technology, its major drawback is its high CO_2 and CO emissions, which are released into the atmosphere and contribute substantially to the greenhouse effect [5].

Methane pyrolysis is an alternate hydrogen generation approach that produces pure hydrogen without CO or CO_2 emissions. This process splits CH_4 directly into its components, i.e., hydrogen and carbon:

$$CH_4 \rightarrow C + 2H_2 \quad (3)$$

During the catalytic methane pyrolysis process, methane is heated to high temperatures (> 750 °C) and converted to hydrogen gas and solid carbon over a catalyst [6]. Currently, the implementation of this process at a commercial scale is not economical due to several process limitations. One limiting factor is the poor catalyst stability at high temperatures and the rapid catalyst deactivation due to the significant solid carbon productions [7]. Another limiting factor is the cost associated with the high energy input required to dissociate CH_4 into H_2 and carbon. Molten salt or molten metal reactor technologies have reached pilot scale development and facilitate in-situ carbon removal; however, they suffer harsh conditions for reactor materials and

the catalysts (salt or metal) must be temperature stable while achieving high catalytic activity [7]. The successful commercialization of methane pyrolysis for CO_2-free H_2 generation requires advanced reactor concepts and improved catalyst formulations to lower the process temperature and manage the co-generated carbon. In addition, generation of high value carbons and their successful recovery can improve the profit margins and make H_2 from methane pyrolysis price competitive with steam methane reforming with carbon capture and storage [8].

Recently, metal catalysts have been considered for methane pyrolysis for their role in reducing the activation energy of C-H bond dissociation. In particular, supported metal catalysts have received much attention as they offer high surface area and porosity compared to non-supported catalysts, which allows for effective dispersion of the active metal particles on the catalyst support [9]. Transition metal catalysts including nickel, iron, and cobalt have been extensively investigated for their excellent catalytic activity originating from their non-filled *3d*-orbital, which promotes hydrocarbon molecule dissociation by partially accepting electrons [9]. Among these, Ni-based and Co-based catalysts have the greatest CH_4 conversion at low temperatures (500-700 °C), with Ni being the most popular choice due to the greater toxicity of Co [7]. Fe-based catalysts have the greatest activity above 700 °C and have been reported to promote carbon nanotube growth [10]. While Ni-based catalysts have excellent catalytic activity for methane decomposition, they suffer from rapid coking from carbon deposition, which quickly deactivates the catalyst [11]. Previous studies have suggested that a bimetallic Ni-Fe-based catalyst can achieve high activity while delaying catalyst deactivation [12-14].

In this study, an advanced reactor concept using microwaves to provide energy to the process and lower the reaction temperature by using microwave-active catalysts is investigated. Microwaves offer a number of advantages over conventional heating including rapid and

104 selective heating, non-contact heating, high energy transfer efficiency, volumetric heating, and
105 rapid startup/shutdown. Microwave-assisted high-temperature reactions have been reported by
106 many researchers to exhibit accelerated reaction rates and/or reduced processing temperatures
107 and selective product formation compared to conventionally heated reactions, which can be
108 hugely beneficial to process efficiency and the economical implementation of high temperature
109 chemical processes [15-18]. Microwaves also enable the use of renewable electricity to drive the
110 process, which is vital for the United States to reach the goal of net-zero carbon emissions by
111 2050 while creating well-paying jobs and growing the economy [19]. Compared to most
112 industrial reactor technologies which require a constant, stable power or fuel supply, the rapid
113 reactor startup and shutdown of microwave reactors enables the use of the variable power
114 outputs supplied by renewable electricity generation.

115 Relatively few studies have investigated microwave catalytic methane pyrolysis to date.
116 Jiang *et al.* compared microwave and thermal heating for methane catalytic pyrolysis over
117 carbon nanotube (CNT)-supported Ni-Pd and Ni-Cu catalysts [20]. Microwave irradiation was
118 reported to enhance catalytic activity compared to thermal heating and the apparent activation
119 energy of the reaction decreased from 45.5 kJ/mol (thermal) to 24.8 kJ/mol (microwave) [20].
120 The same group investigated the Ni-Pd/CNT catalyst under hybrid microwave and thermal
121 heating and reported a 60% reduction of the power required to maintain the methane pyrolysis
122 reaction temperature compared to microwave heating alone, demonstrating a design for
123 improved reactor efficiency [21]. Dadsetan *et al.* used a microwave reactor with fluidized
124 carbon pellets reaching temperatures in excess of 1200 °C [22]. The study demonstrated stable
125 methane conversion over 500 cumulative hours of testing with over 90% hydrogen selectivity at
126 temperatures greater than 1000 °C [22]. While several studies exist on microwave-based

127 catalytic methane pyrolysis, further research is needed to investigate different microwave-active
128 catalysts and process conditions to optimize catalyst activity, catalyst stability, and process
129 energy efficiency.

130 The specific interaction of microwave energy with materials is an important consideration
131 to guide catalyst selection. For microwave heating of heterogeneous catalysts, different phases
132 within the catalyst material (e.g., metal particles, support material, pores/void spaces) experience
133 different microwave absorption, depending on their material dielectric properties. As a result,
134 different heating rates of different materials within the catalyst material may be achieved by
135 microwave selective heating leading to formation of hotspots. For example, metallic particles
136 exhibit excellent microwave absorption due to their conductivity and may reach greater
137 temperatures than its surroundings (support and void spaces) [23, 24]. Hotspot formation can
138 enhance heterogeneous catalyst performance by selectively heating active metallic particles to
139 reaction temperatures while minimizing power absorption in the inactive materials of the
140 catalyst. However, excessive heating can also lead to metal particle melting or crystallization,
141 which can negatively impact catalyst performance [25]. For methane pyrolysis, hotspot
142 formation on metallic active sites can accelerate methane activation while keeping bulk
143 temperatures lower to prevent coke formation [26]. By targeting heating on the metal sites,
144 microwave selective heating has the potential to improve energy efficiency. In addition, micron-
145 scale plasma discharges (microplasmas) can occur when the electric field is concentrated
146 between absorptive particles that are close together. Zhang et al.(2023) studied the microplasma
147 discharge characteristics on carbon catalysts and suggested that high intensity discharges could
148 promote activation and decomposition of reactant gas species during microwave CO_2 reforming
149 of methane [27].

The existing literature on microwave methane pyrolysis have mainly investigated carbon-based catalyst materials as a microwave absorber/heat carrier without addition of metal species to enhance methane decomposition [22, 28, 29]. The number of studies that have investigated supported metal catalysts for microwave methane pyrolysis is extremely scarce and the scope of catalysts tested to date is limited [20, 21]. Therefore, further work is needed to explore different catalyst systems that are well suited for microwave methane pyrolysis. As catalyst cost is one factor that drives process economics [8], the present study aims to investigate low-cost catalyst systems that can be attained by scalable synthesis methods that would be practical for microwave methane decomposition at a large scale.

The present study investigates the catalytic performance of monometallic Ni and Fe and bimetallic Ni-Fe catalysts supported on activated carbon for microwave methane pyrolysis, which represents a low-cost catalyst system that may be attractive for commercial adoption of this technology. While activated carbon supported Ni, Fe, and Ni-Fe catalysts have been well studied during conventional methane pyrolysis, they have not been investigated for microwave methane pyrolysis to our knowledge. Nickel was chosen for its good reactivity for C-H bond cleavage while iron is a low-cost, earth-abundant catalyst that may promote carbon nanotube formation [30]. The activated carbon support was chosen for its high surface area and stability, which ensures effective dispersion of the supported metals on the support and the longevity of the catalysts [31]. Activated carbon has many additional benefits, such as its initial low cost, high mechanical resistance, good reductive properties, and the fact that it is susceptible to microwave heating [30, 31].

2. Experimental

2.1 Materials

Granular activated carbon (Calgon) was used as the support material, nickel nitrate hexahydrate (Ni $(NO_3)_2 \cdot 6H_2O$, Alfa Aesar) was used as the Ni precursor, and iron nitrate nonahydrate ($Fe(NO_3)_3 \cdot 9H_2O$, Sigma-Aldrich) was used as the Fe precursor. The granular activated carbon (AC) was ball milled to a fine powder before the preparation of the catalysts.

2.2 Catalyst synthesis methods

A wet impregnation method was utilized to synthesize the supported metallic catalysts on activated carbon. The wet impregnation method is by far the most widely used method for the preparation of heterogeneous catalysts as it is simple to achieve technically, has relatively low costs, and can be scaled-up easily. Generally, a support material is impregnated with a solution containing a precursor and subsequently dried [32].

The single metallic catalysts were prepared by wet impregnation of nickel and/or iron on the activated carbon support to achieve a 30 wt% metals loading. For 10 g activated carbon, 37.84 g of Ni $(NO_3)_2 \cdot 6H_2O$ or 43.41 g $Fe(NO_3)_3 \cdot 9H_2O$ was dissolved in 100 mL of solvent (75 mL of distilled water and 25 mL of ethanol). The bimetallic catalyst was prepared with a 1:1 molar ratio of nickel and iron with total metal loading of 30% wt, i.e., 15% wt Ni and 15% wt Fe. For 20 g of activated carbon, 22.3 g of $Ni(NO_3)_2 \cdot 6H_2O$ and 32.6 g $Fe(NO_3)_3 \cdot 9H_2O$ were dissolved in 120 mL of solvent (100 mL distilled water and 20 mL of ethanol). Activated carbon was added to the single and bi-metallic precursor solutions, then held at 60 °C under constant stirring for 6-12 hours until the solvent had evaporated. The catalysts were dried at 100 °C overnight and calcined at 350 °C for 4 hours with a heating rate of 5 °C/min, then ground to a fine powder.

Before reaction testing, the prepared catalysts were reduced in a flow-through fixed-bed reactor. The catalysts were reduced at 500 °C under 150 sccm flow of 100% H_2 and held for 3

hours, followed by passivation at room temperature under 150 sccm flow of 1% O_2/N_2 for 6 hours. The reduction temperature was selected based on published methodologies from experimental synthesis of similar Ni-, Fe-, and NiFe- based catalysts [33]. The activated carbon is referred to as AC, while the reduced metal supported catalysts are referred to as Ni/AC, Fe/AC, and Ni-Fe/AC in this paper.

2.3 Microwave reaction testing methodology

A flow-through microwave reactor was utilized for catalytic methane pyrolysis reaction testing of the powder catalysts (Figure 1). The reduced catalyst in powder form was supported on a piece of quartz wool in the center of a quartz tube (14 mm ID) and placed inside a rectangular waveguide applicator (WR340). The reactor was powered by a 2 kW, 2.45 GHz power supply with continuous wave output (GMP20K, Sairem) and was equipped with an auto-tuner for impedance matching. An automated sliding short was used to maximize the microwave-material coupling by adjusting the short position to ensure the peak E field was positioned on the catalyst bed, which also ensures reproducibility. Temperature measurement by an IR sensor (Impac, Advanced Energy) with a spectral range of 2.3 μm allowed temperature determination of the catalyst bed surface, just inside the quartz tube. The reaction temperature was controlled by a PLC that adjusted the duty cycle of microwave pulsing from the source to maintain the setpoint temperature. Forward and reflected power were continuously measured during each microwave test. The mean power absorbed by the catalyst was estimated as the difference in forward and reflected power, which was averaged over the duration of each run.

For comparison, a conventional heating test was run for the bimetallic catalyst using an electric furnace. The conventional reactor consisted of a reactor tube heated by an electric

furnace with catalyst bed temperature measurement by K-type thermocouple. The conventional heating test was run under the same experimental conditions as the microwave tests at 800 °C.

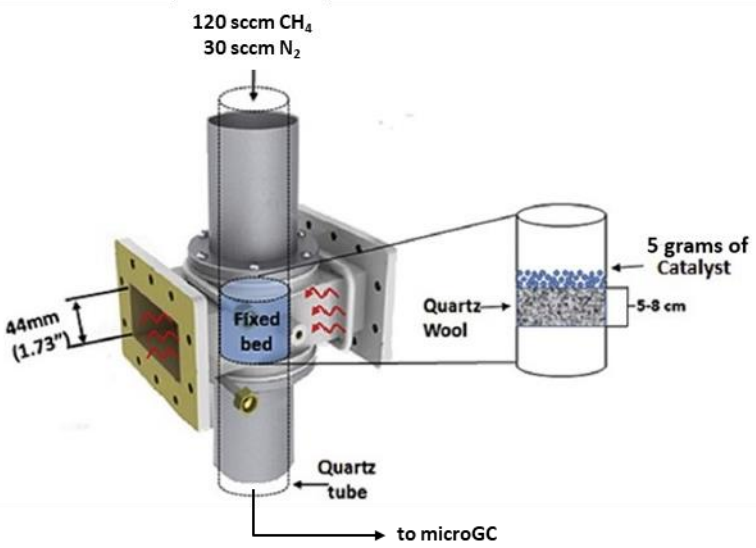

Figure 1. Schematic of microwave reactor (adapted from [34])

Eight microwave tests and one conventional heating test were conducted to study the hydrogen yields from catalytic methane pyrolysis. For the microwave tests, each catalyst was reacted at 600 °C and 800 °C, while the conventional test was only carried out with the bimetallic Fe-Ni/AC catalyst at 800 °C. For each experimental test, 5 grams of powdered catalyst was added to the quartz reactor tube, held in place with quartz wool, and placed at the center of the microwave reactor. The catalyst was preheated to the reaction temperature (600 °C or 800 °C) under 150 sccm nitrogen before starting the flow of 120 sccm methane and 30 sccm nitrogen. It is known that methane flow rate is inversely proportional to hydrogen yield in catalytic methane pyrolysis due to the reduced methane contact time with increasing flows [1, 9]. The dilution with N_2 would not be necessary for commercial implementation and was only added as an internal standard for gas analysis. Further, the typical gas hourly space velocity (GHSV)

used during testing was approximately 1740 h^{-1}, which is on the low end of the range of GHSVs reported in previous publications to maximize contact time [9, 26]. During the reaction, the gas composition of the reactor effluent was analyzed on-line by gas chromatography (3000A micro GC, Agilent Technologies) equipped with a TCD detector and four columns: molecular sieve 5˚A, Plot Q, Plot U, and Alumina, and capable of detecting N_2, CH_4, H_2, CO, CO_2, and C_2-C_6 hydrocarbons. The reaction duration was 60 minutes from the time methane was first introduced into the reactor, and each test was repeated in duplicate to ensure repeatability.

The methane conversion (X_{CH4}) was calculated according to Equation 4:

$$X_{CH4}(\%) = \frac{mol\ CH_{4\ in} - mol\ CH_{4\ out}}{mol\ CH_{4\ in}} * 100\% \quad (4)$$

where $mol\ CH_{4\ in}$ and $mol\ CH_{4\ out}$ represent the moles of methane fed into the reactor and the moles of unreacted methane in the effluent, respectively. Mean methane conversion was determined as the average of transient methane conversion values obtained over the duration of each experiment. The mean percent hydrogen yield (X_{H2}) from each reaction test was calculated by Equation 5 :

$$X_{H2}(\%) = \frac{mol\ H_{2\ out}}{mol\ CH_{4\ in} * 2} * 100\% \quad (5)$$

where $mol\ H_{2\ out}$ represents the moles of H_2 gas in the effluent. Solid carbon yield ($X_{C,solid}$) was calculated according to Equation 6, then the transient yields were integrated over the reaction time:

$$Carbon\ Yield\ (g/100\ g\ catalyst) = \frac{mass\ C\ in - mass\ C\ out}{100 *\ mass\ catalyst} \quad (6)$$

where *mass* C_{in} represents the mass of elemental carbon in the methane fed into the reactor and *mass* C_{out} represents the mass of elemental carbon in the effluent gas species. H_2 selectivity (S_{H2}) was calculated according to Equation 7:

$$S_{H2}(\%) = \frac{mol\ H_{2\ out}}{mol\ C_x H_{y\ out}} \quad (7)$$

where *mol* $C_xH_{y\ out}$ represents the moles of H-containing species in the effluent, excluding unreacted methane.

2.4. Catalyst characterization

Catalysts were characterized by several techniques before and after reaction. Before reaction testing, x-ray diffraction (XRD) of the pre-reduced, reduced, and post-reaction catalysts was carried out on a PANalytical X'Pert Pro equipped with a Cu tube maintained at 45 kV and 40 mA and a vertical circle theta:theta goniometer with a radius of 240mm. This design allows for high-speed data collection while keeping the sample in a horizontal position during data collection. X-ray diffractograms were collected with 2θ from 10° to 75° and a step size of 2.67°. Diffractogram data were analyzed using the *HighScore* software. Scanning electron microscopy (SEM) (Thermo-Scientific Apreo-2C) was used to investigate the morphology of spent catalysts after the microwave reaction. Thermogravimetric analysis (TGA) of the fresh and spent metal catalysts after methane pyrolysis at 800 °C was carried out on a Discovery TGA (TG Instruments). The mass loss data was collected during heating from 120 to 900 °C at 5 °C/min from 120 to 900 C under oxidative conditions (25 mL/min air).

3. Results and Discussion

3.1 Microwave reaction data analysis

Figure 2 shows the transient product yields during catalytic methane pyrolysis. The metal-supported catalysts showed better overall catalytic activity than the AC catalyst, and in all cases, more H_2 is produced at 800 °C than at 600 °C. During the course of the reaction, the yield of H_2 and methane conversion generally decreases during each test, which is due to the formation and accumulation of solid carbon on the catalyst, decreasing the catalyst activity over time. Peak formation in the transient gas yield data observed for the Fe/AC catalyst at 800 °C is attributed to a temporary pressure instability that occurred during the experimental test. Trace gases, namely CO, CO2, ethane, and ethylene, were detected by the microGC during methane pyrolysis experiments and their transient yields are shown in Figure 3.

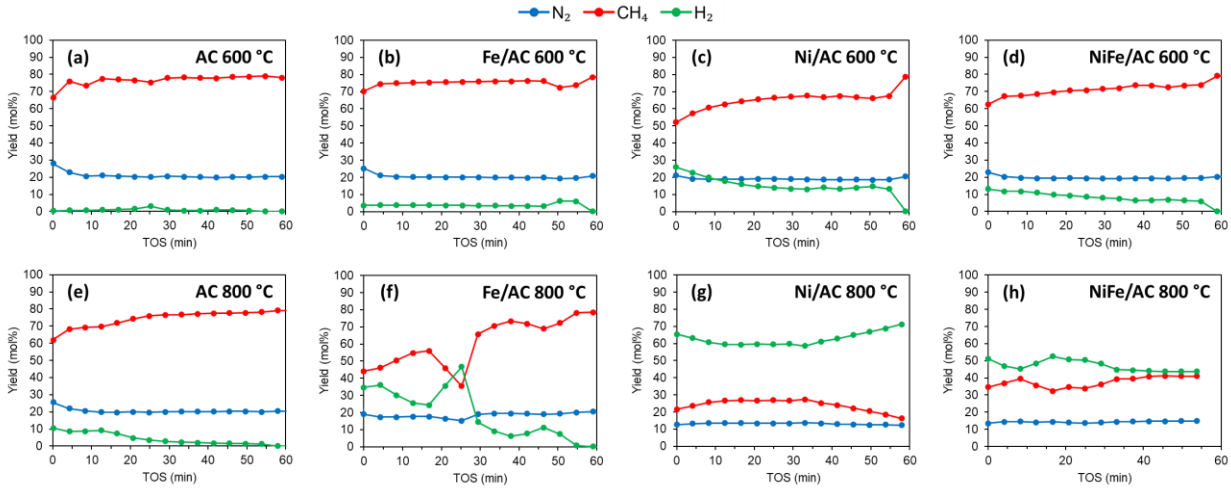

Figure 2. Transient gas yields during catalytic methane pyrolysis for each catalyst at 600 °C (a-d) and 800 °C (e-h)

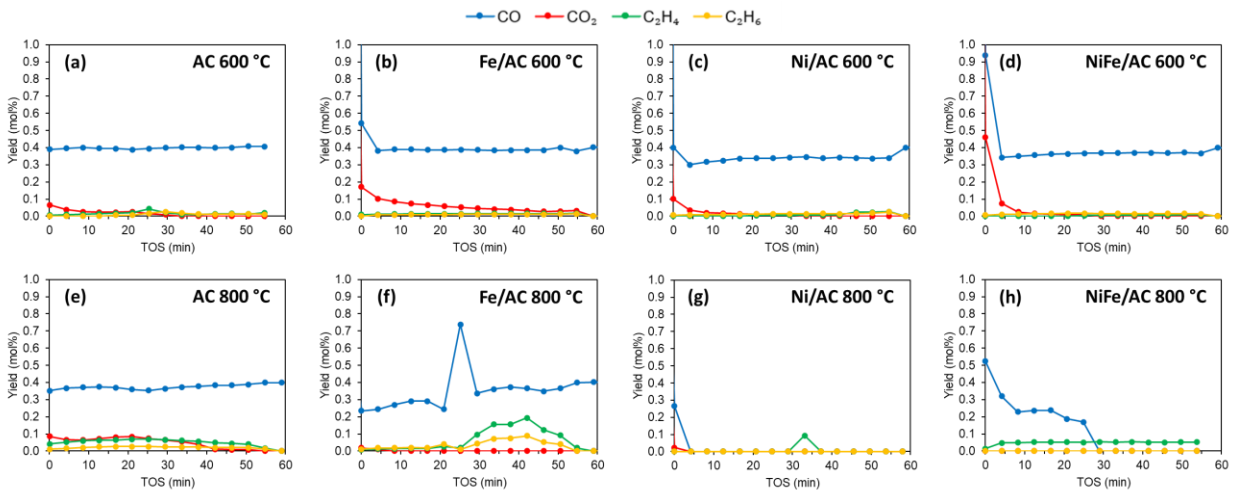

283

284 Figure 3. Transient trace gas yields (CO, CO_2, C_2H_4, C_2H_6) during catalytic methane pyrolysis

285 for each catalyst at 600 °C (a-d) and 800 °C (e-h)

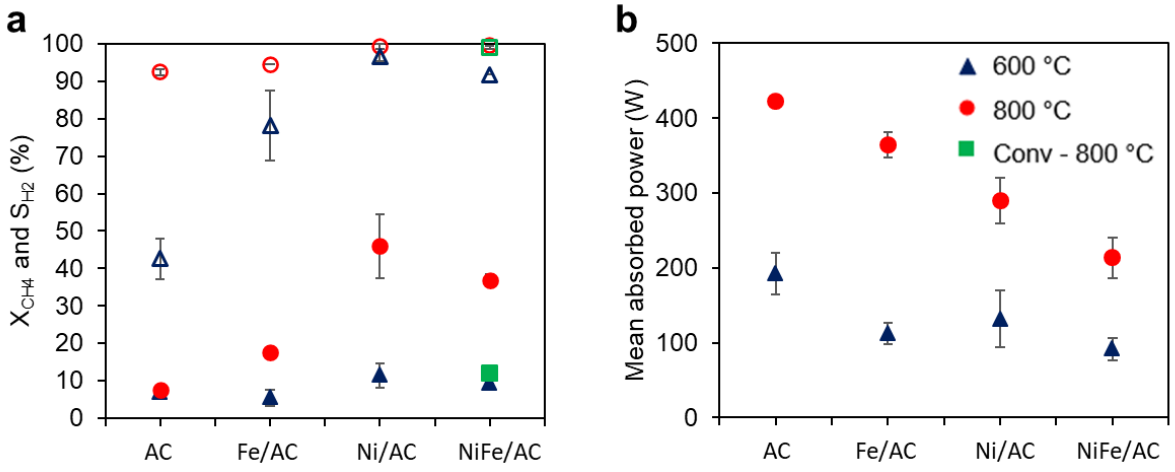

286

287

288 Figure 4. (a) Mean methane conversion, X_{CH4}, at 600 °C (▲) and 800 °C (●) and hydrogen

289 selectivity, S_{H2}, at 600 °C (△) and 800 °C (○) for each catalyst during microwave methane

290 pyrolysis and conventional methane pyrolysis with NiFe/AC at 800 °C (X_{CH4}: ■ and S_{H2}: □) and

291 (b) mean absorbed power during microwave methane pyrolysis for each catalyst at 600 and

292 800 °C

293 Figure 4a shows the mean methane conversion (X_{CH4}) and mean hydrogen selectivity
294 (S_{H2}) during catalytic methane pyrolysis. Microwave methane pyrolysis with the Ni/AC catalyst
295 at 800 °C had the greatest CH_4 conversion of 46.0%, and a slightly lower conversion level of
296 36.9% was observed for the bimetallic catalysts at 800 °C. H_2 selectivity showed some variation
297 for the different catalysts and test conditions studied. For the reaction at 600 °C, the H_2
298 selectivity was lower than at 800 °C for all catalysts. For AC and Fe/AC catalysts at 600 °C, the
299 H_2 selectivity was 42.6 and 78.1%, respectively, while Ni/AC and Ni-Fe/AC reached > 90% H_2
300 selectivity at 600 °C. The main trace gas species co-produced were CO, ethane, and ethylene for
301 the metal-supported catalysts; however, for tests with the AC catalyst, CO_2 was the main co-
302 produced gas species, which could be a result of possible decomposition of the oxygen
303 containing species on the catalyst itself at the reaction temperatures tested since this was the only
304 catalyst that was not reduced. For methane pyrolysis at 800 °C, the H_2 selectivity significantly
305 increased, with all catalysts reaching >90% selectivity and Ni/AC and NiFe/AC reaching >99%.
306 Methane pyrolysis under conventional heating with the NiFe/AC catalyst at 800 °C had a similar
307 H_2 selectivity (>99%) compared to the microwave pyrolysis tests at the same temperature;
308 however, the CH_4 conversion was only 12.1% compared to 36.9% under microwave irradiation
309 at the same temperature. Microwave-assisted methane pyrolysis increased the methane
310 conversion by 3-fold compared to conventional heating.

311 Based on Figure 4b, the power absorbed during microwave tests differed for each
312 catalyst, with the AC having the most significant power absorption, indicating that this catalyst
313 needed the most power to maintain the reaction temperature. With the addition of metallic
314 species to the AC support, the power required decreased, indicating better microwave heat
315 transfer efficiency, which supports selective heating of the metallic phases. Interestingly, the

316 bimetallic catalyst had the lowest power requirement than either the Fe/AC or Ni/AC catalyst,
317 which indicates that the Ni-Fe bimetallic complexes improved the microwave coupling
318 compared to single metal Fe or Ni catalysts. Perhaps the bimetallic Ni-Fe complexes introduced
319 a heterogeneous charge distribution compared to the single metal catalysts, which increased the
320 interfacial polarization effects leading to increased microwave absorption; however, the
321 dielectric loss mechanism was not explored further in this study. It should be noted that in all
322 cases, the absorbed power was greater than 90% of the microwave input power, indicating that
323 each of the catalysts had excellent microwave heating ability owing to the carbon support and
324 metal particles.

325 Based on the mean hydrogen gas yield reported in Figure 4a, it was observed that the
326 monometallic Ni/AC catalyst had a substantially higher hydrogen yield than Fe/AC for both
327 tested temperatures, while the AC catalyst had the lowest hydrogen yield, corresponding to the
328 same trends observed for CH4 conversion, as expected. The Ni/AC catalyst during microwave
329 methane pyrolysis at 800 °C had the highest hydrogen yield at 46.9%, while the bimetallic
330 catalyst had a slightly lower hydrogen yield of 40.5%. This value can be directly compared to the
331 conventional reactor heating method, which also took place at 800 °C with the bimetallic catalyst
332 and yielded 15.8% H_2, which is less than half of the hydrogen yielded in the microwave reactor.
333 It is possible that the differences in hydrogen yield percentage were caused by the non-uniform
334 distribution of the electromagnetic field within the catalyst bed [15]. Microwave energy has a
335 susceptibility to selectively couple to metallic sites, which produces a temperature gradient
336 between the catalyst support and metal sites. This means that the localized temperatures of the
337 catalyst metal sites may have reached greater than the 600 °C or 800 °C setpoint temperature
338 during microwave heating, therefore increasing the reaction rate above the reaction rate expected

339 at that temperature based on the reaction thermodynamics. The solid carbon yields (Figure 4b)
340 were generally proportional to the H_2 yields during catalytic methane pyrolysis, with the tests
341 having the greatest H_2 yield producing the greatest yield of carbon. While Ni/AC was the most
342 active catalyst for methane decomposition, it suffered the most from solid carbon deposition
343 leading to rapid catalyst deactivation. The Fe/AC and NiFe/AC, on the other hand, had slightly
344 lower catalytic activity but resisted carbon formation, which may suggest that the bimetallic
345 catalyst would have better long-term performance. As the catalysts were only tested for a 60-
346 minute duration, further study is needed to analyze the long-term performance of each catalyst
347 and weigh the tradeoff between catalytic activity and solid carbon formation and accumulation
348 on the catalyst. Table 1 presents the carbon balance including the amount of input carbon
349 sources (CH_4) and amounts of individual output carbon sources (unreacted CH_4, CO, CO_2, C_2H_4,
350 and C_2H_6) that were used to estimate the carbon yields reported in Figure 5b.
351

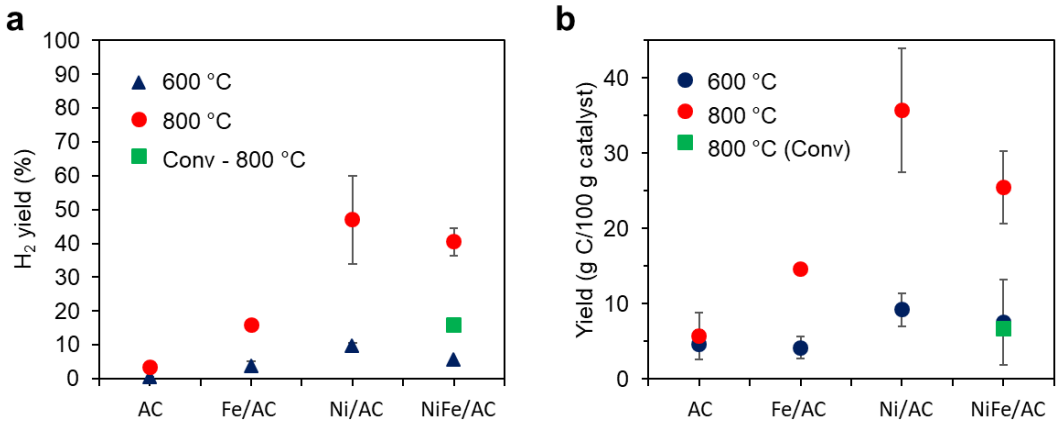

352
353 Figure 5. (a) H_2 yield and (b) solid carbon yield for each catalyst after methane pyrolysis at
354 600 °C and 800 °C.
355

Table 1: Carbon balance for each reaction condition (all standard deviations are <5% of the reported values)

Catalyst	C_{input} (mmol C / g)	$C_{Outputs}$ (mmol C / g)						C Yield (mmol C / g)	C Yield (g C / 100 g catalyst)
	C_{CH4}	C_{CH4}	C_{CO}	C_{CO2}	C_{C2H4}	C_{C2H6}	Total		
AC – 600 °C	62.6	58.5	0.2	0.0	0.0	0.0	58.7	3.8	4.6
AC – 800 °C	69.3	64.1	0.2	0.0	0.1	0.1	64.5	4.8	5.7
Fe/AC – 600 °C	71.6	67.7	0.3	0.1	0.0	0.0	68.1	3.5	4.2
Fe/AC – 800 °C	72.2	59.5	0.3	0.0	0.1	0.1	60.1	12.2	14.6
Ni/AC – 600 °C	71.6	63.6	0.2	0.0	0.0	0.0	63.9	7.7	9.2
Ni/AC – 800 °C	64.8	34.9	0.2	0.0	0.0	0.0	35.1	29.7	35.7
NiFe/AC – 600 °C	72.2	65.5	0.4	0.0	0.0	0.0	66.0	6.3	7.5
NiFe/AC – 800 °C	67.8	45.7	0.9	0.0	0.1	0.0	46.6	21.2	25.5
NiFe/AC – 800 °C (conv)	63.6	57.9	0.0	0.0	0.1	0.0	58.0	5.6	6.7

3.2 Catalyst characterization

3.2.1 XRD analysis

The XRD diffractograms of the pre-reduced and reduced catalysts help with phase identification of the material and the crystallographic structure determination (Figure 6). It is evident by analyzing the characteristic diffraction patterns that nickel and iron oxides are present in all catalysts before reduction, whereas the activated carbon has broad peaks ascribed to amorphous carbon at 26° and 42°. In the pre-reduced NiFe/AC catalyst, a $NiFe_2O_4$ phase is observed in the XRD data, which has been previously reported for non-reduced NiFe supported catalysts prepared by wet impregnation [14, 35]. It is also noted that Ni metal is observed in the pre-reduced Ni/AC X-ray diffractograms; however, the reason is not clear. Except for some small iron oxide peaks for the reduced Fe-AC catalyst, the metal oxides were reduced to metallic nickel and iron, indicating that the reduction process successfully reduced the oxides to

catalytically active metals. The bimetallic catalyst shows characteristic diffraction peaks of both Ni-Fe alloy and Ni metal, which is consistent with previous studies [14].

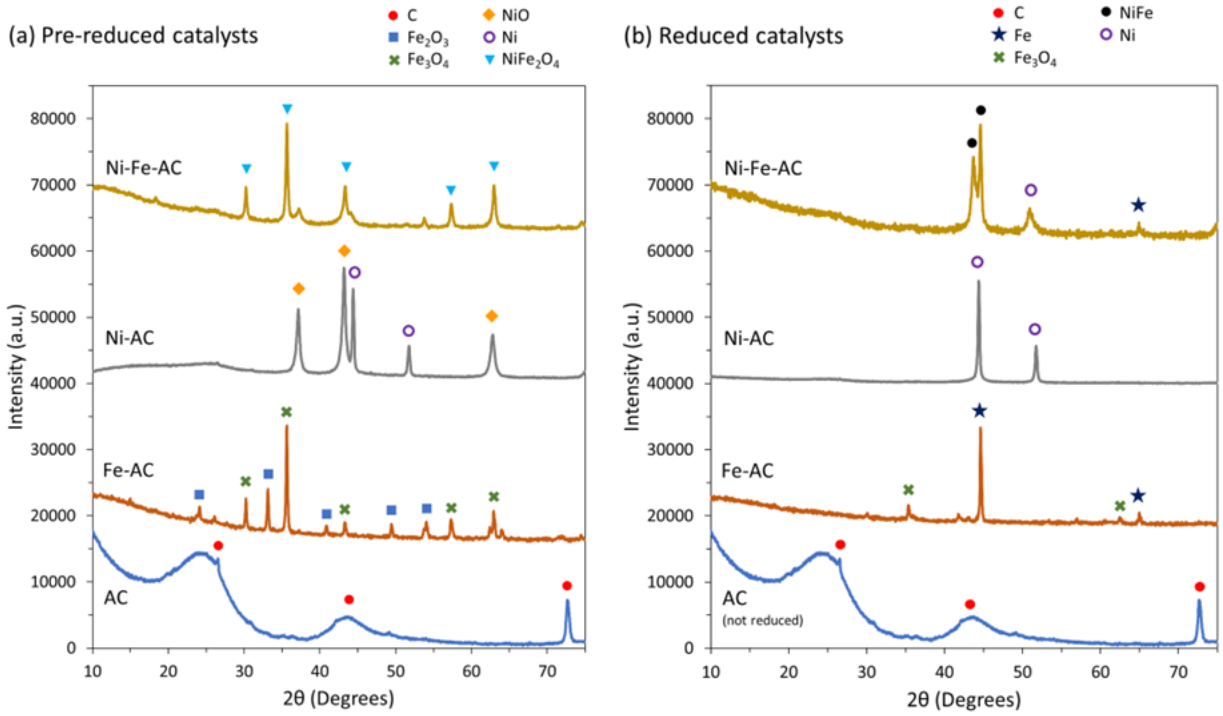

Figure 6. X-ray diffractograms of (a) pre-reduced and (b) reduced catalysts

The XRD results from the post-reaction catalysts runs at 600 °C and 800 °C can be found in Figure 7, with each diffraction peak labeled. There is evidence that carbon formed during the microwave reactor runs on the bimetallic Ni-Fe/AC and the Ni/AC catalysts, which had the greatest carbon yields according to Figure 5b. The Fe-based catalyst on the other hand had a lower carbon yield and no clear carbon peaks could be seen from XRD of the Fe-based catalyst. It is believed that the small but sharp carbon peaks in the x-ray diffractograms could be attributed to some type of graphitic carbon, which has a characteristic diffraction peak around $2\theta = 27$ [36]. However, more investigation is needed to be certain of that assignment, as XRD testing is primarily used for bulk analysis. By completing XRD on the post-reaction catalysts, it can be

384 concluded that the resultant catalysts most likely suffered changes to their structural properties,
385 indicating that the microwave reactor influenced catalytic performance.

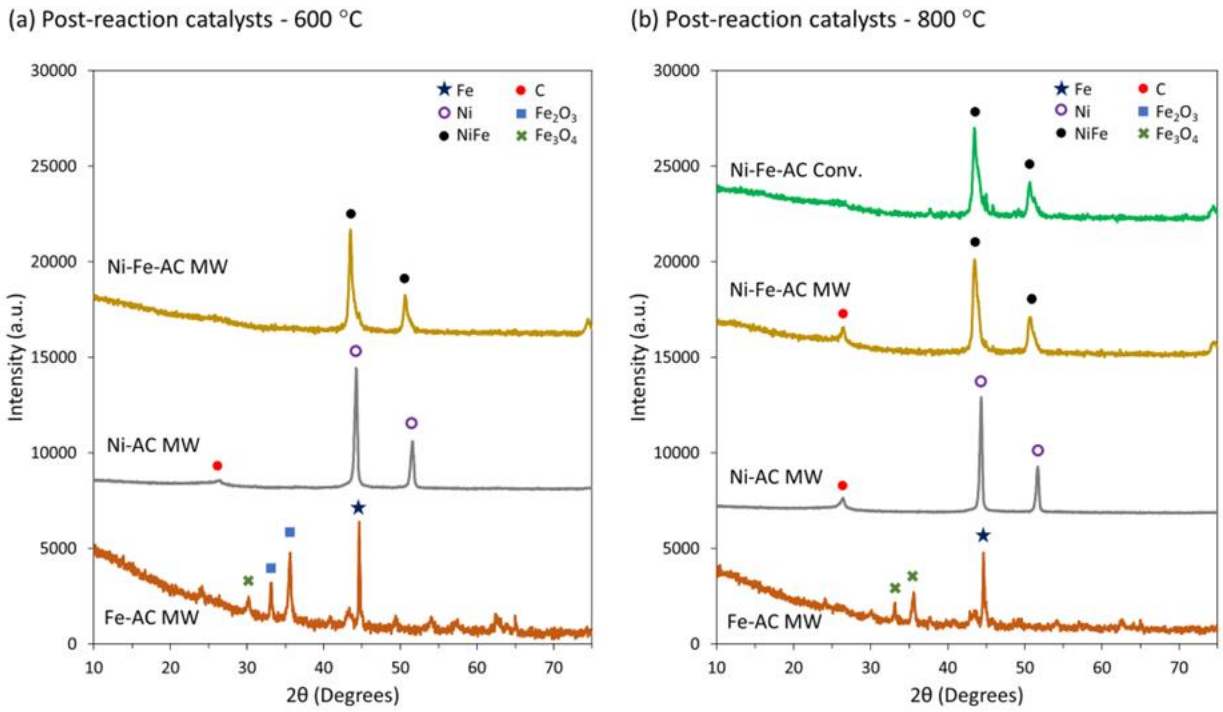

386

387 Figure 7. X-ray diffractograms of post-reaction catalysts at (a) 600 °C and (b) 800 °C.

388 **3.2.2 SEM imaging**

389 To investigate the morphology of the formed carbon, the spent catalysts were analyzed by
390 SEM (Figure 8). . Spherical particles are observed on the spent Fe/AC and bimetallic Ni-Fe/AC,
391 which are most likely the metallic catalyst particles. These catalysts had lower carbon yield that
392 the Ni/AC and the presence of formed carbon is not apparent in the images. The carbon may be
393 deposited as a thin coating on the metallic particle surfaces, which could inhibit the methane
394 decomposition reaction and may be a reason for the lower catalytic activity of the Fe/AC and Ni-
395 Fe/AC catalysts compared to Ni/AC. Filamentous carbon is observed on the spent Ni/AC. The

396 filamentous carbon morphology on Ni/AC allows greater availability of metal sites for methane
397 decomposition reactions. Filamentous carbon formation is commonly reported during methane
398 decomposition with Ni-based catalysts.

399

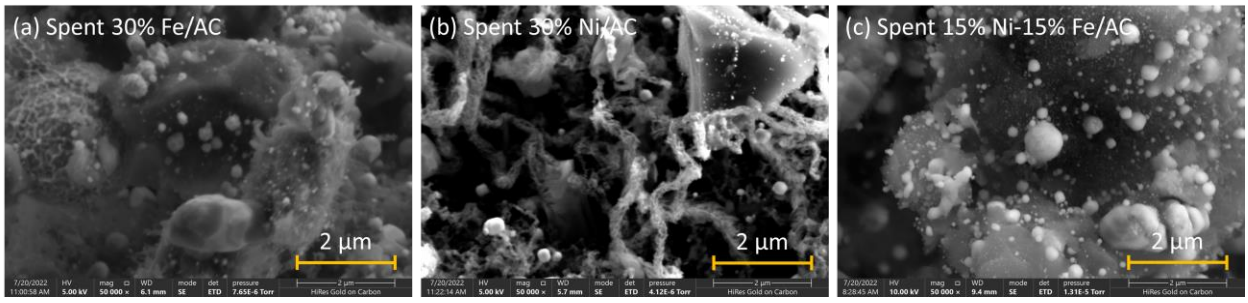

400

401 **Figure 8.** SEM images of spent catalysts at 50,000x field magnification (a: Fe/AC), b: Ni/AC, c:
402 Ni-Fe/AC).

403

404 It was interesting to discover evidence of carbon filaments/nanotubes on the spent 30%
405 nickel catalyst, as illustrated in Figure 9. This result agrees with the X-ray diffraction results that
406 also showed the existence of carbon on the nickel catalyst. Carbon nanotubes have become a
407 widely investigated research field since its discovery in 1991 by S Ijima [37]. They are a high-
408 value carbon product that can add economic value when coproduced during a catalytic process.
409 Carbon nanotubes are very lightweight while presenting toughness, flexibility, high surface area
410 and good electric conductivity. Because of these characteristics, carbon nanotubes can be made
411 into high-strength composites and can be applied to different industries [37] . Also, carbon
412 nanotubes have both conductor and semiconductor properties making them even more valuable
413 for the development of microelectronics. A recent technoeconomic analysis of methane pyrolysis
414 processes showed that sale of co-produced carbon products such as carbon black and graphitic

carbon can produce H_2 with a high profit margin [8]. Depending on the carbon selling price, H_2 from methane pyrolysis can be potentially more profitable than H_2 produced from steam reforming with carbon capture and storage [8]. Therefore, the discovery of this carbon nano-tube co-product is exciting from an economic standpoint and one that should be investigated further.

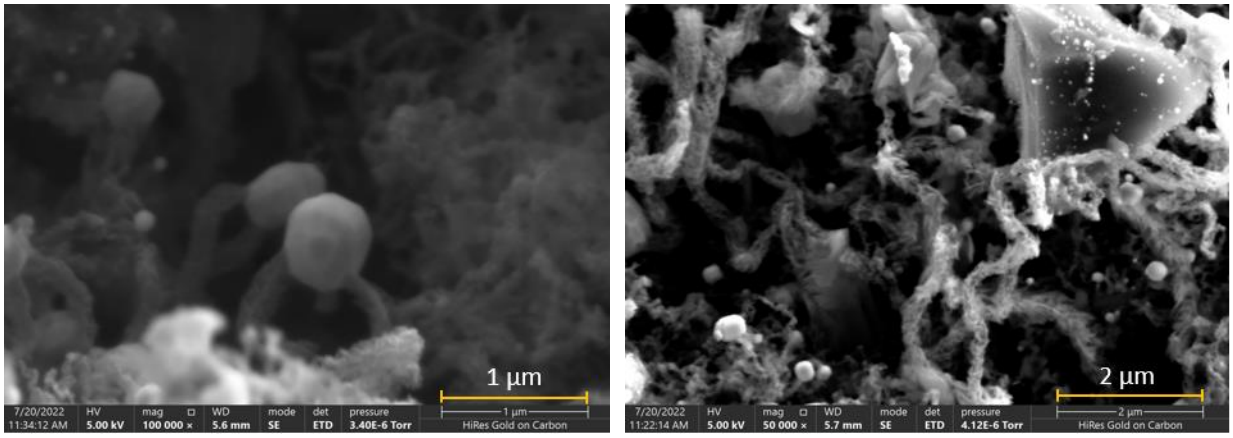

Figure 9. SEM images of spent 30% Ni/AC catalysts with evidence of carbon filaments/nanotubes

3.2.3 TGA

The thermal decomposition behavior of fresh and spent catalysts during combustion was analyzed by TGA (Figure 10). The mass loss during decomposition represents the total carbon in the sample, while the final mass represents the inorganic matter from the supported metals and residual ash from the activated carbon support. The difference in mass loss between the fresh and spent catalyst was calculated to estimate the amount of solid carbon formed during the reaction and the mass loss data is summarized in Table 2. The estimated carbon yields from microwave methane pyrolysis at 800 °C are 5.1, 22.0, and 9.3 for the Fe/AC, Ni/AC, and NiFe/AC catalysts, respectively. These estimates are lower than those previously estimated by carbon balance (based on GC data) for the same experiments, which were 14.6, 35.7, and 25.5

for the Fe/AC, Ni/AC, and NiFe/AC catalysts at 800 °C, respectively. This discrepancy suggests that some carbon may have deposited on the reactor walls. As none was observed on the walls of the quartz reactor tube after each experiment, some carbon may have deposited downstream of the reactor.

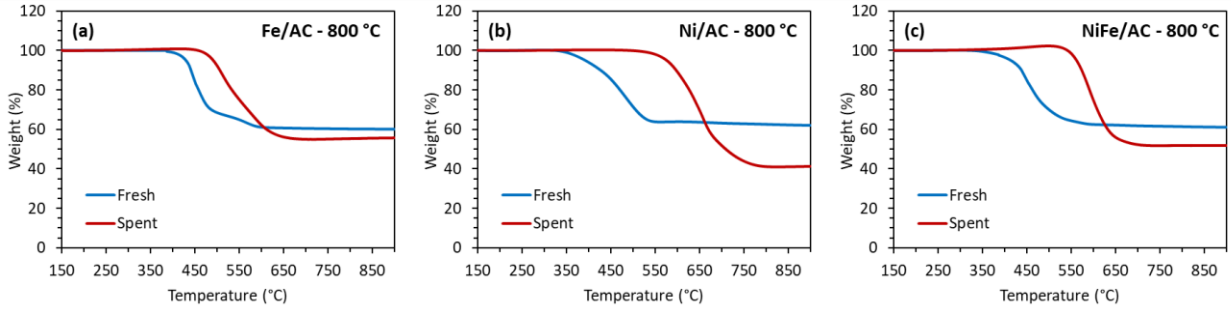

Figure 10: TG curves of fresh and spent metallic catalysts from microwave methane pyrolysis at 800 °C (a: Fe/AC, b: Ni/AC, and c: NiFe/AC).

Table 2: Mass loss and carbon yield determined from TGA of fresh and spent metallic catalysts from microwave methane pyrolysis at 800 °C

Catalyst	Mass loss (%)		Residue (%)		Carbon yield[a] (g C/100 g catalyst)
	Fresh	Spent	Fresh	Spent	
Fe/AC – 800 °C	39.8	44.9	60.2	55.1	5.1
Ni/AC – 800 °C	37.9	59.9	62.1	40.1	22.0
NiFe/AC – 800 °C	38.8	48.1	61.2	51.9	9.3

[a] Determined by Carbon yield (g C/100 g catalyst) = Mass loss, spent – Mass loss, fresh

4. Conclusions

The monometallic and bimetallic catalysts supported on activated carbon were prepared using wet impregnation, followed by the reduction of metal oxides to metallic Fe, Ni and Ni-Fe. It is evident that heating with microwave energy improved the catalytic activity for methane

pyrolysis. Compared to conventional heating with the bimetallic Ni-Fe/AC catalyst, there was a three-fold increase in hydrogen yield and methane conversion under microwave irradiation at the same reaction temperature (800 °C), which is attributed to hotspot formation at the metal active sites, for example. Out of all the catalysts, the bimetallic Ni-Fe/AC catalyst is the most promising for its high activity and longer stability by resisting deactivation by carbon deposition. Another significant finding is the formation of filamentous carbon in the spent 30% Ni/AC catalyst. This co-product could add economic value at commercial scale and allow for more industries to utilize methane pyrolysis.

This study provides valuable insights on the microwave methane decomposition on activated carbon supported Fe, Ni, and NiFe catalysts and serves as a foundation to guide future catalyst and reaction optimization. More in-depth characterization of the pre-and post-reaction catalysts is needed to understand carbon formation mechanisms and longer term experimental testing could help understand catalyst deactivation during longer times-on-stream. A comprehensive optimization of the bimetallic catalyst composition (e.g., Ni/Fe ratio, support material, etc.) and the microwave methane pyrolysis reaction conditions is needed to improve the catalytic performance, microwave power utilization, and overall energy efficiency. As catalyst deactivation was observed during the 60 minute reaction time considered in this study, it would also be interesting to investigate ways to improve the catalyst longevity of the monometallic and bimetallic catalysts, either by the addition of promoters to the catalyst or by process optimization.

5. Declaration of Competing Interest

There was no conflict of interest at the time this paper was written.

6. Acknowledgments

JL would like to sincerely thank the Mickey Leland Energy Foundation for giving her the opportunity to work with such talented researchers at the National Energy Technology Laboratory in Morgantown, WV. We would also have not been able to complete data collection without research technicians Gregg Sell and Donald Floyd.

7. Disclaimer

This project was funded by the United States Department of Energy, National Energy Technology Laboratory, in part, through a site support contract. Neither the United States Government nor any agency thereof, nor any of their employees, nor the support contractor, nor any of their employees, makes any warranty, express or implied, or assumes any legal liability or responsibility for the accuracy, completeness, or usefulness of any information, apparatus, product, or process disclosed, or represents that its use would not infringe privately owned rights. Reference herein to any specific commercial product, process, or service by trade name, trademark, manufacturer, or otherwise does not necessarily constitute or imply its endorsement, recommendation, or favoring by the United States Government or any agency thereof. The views and opinions of authors expressed herein do not necessarily state or reflect those of the United States Government or any agency thereof. USDA is an equal opportunity provider and employer.

References

[1] N. Sánchez-Bastardo, R. Schlögl, H. Ruland, Methane Pyrolysis for CO2-Free H2 Production: A Green Process to Overcome Renewable Energies Unsteadiness, Chemie Ingenieur Technik, 92 (2020) 1596-1609.
[2] T.W.H.B. Room, FACT SHEET: President Biden Signs Executive Order Catalyzing America's Clean Energy Economy Through Federal Sustainability, 2021.
[3] U.S.D.o. Energy, Hydrogen Fuel Basics, 2022.

[4] A. Basile, S. Liguori, A. Iulianelli, 2 - Membrane reactors for methane steam reforming (MSR), in: A. Basile, L. Di Paola, F.l. Hai, V. Piemonte (Eds.) Membrane Reactors for Energy Applications and Basic Chemical Production, Woodhead Publishing2015, pp. 31-59.
[5] S. Energy, Steam Methane Reforming, 2018.
[6] H.M. Nguyen, J. Sunarso, C. Li, G.H. Pham, C. Phan, S. Liu, Microwave-assisted catalytic methane reforming: A review, Applied Catalysis A: General, 599 (2020) 117620.
[7] M. McConnachie, M. Konarova, S. Smart, Literature review of the catalytic pyrolysis of methane for hydrogen and carbon production, International Journal of Hydrogen Energy, (2023).
[8] J. Riley, C. Atallah, R. Siriwardane, R. Stevens, Technoeconomic analysis for hydrogen and carbon Co-Production via catalytic pyrolysis of methane, International Journal of Hydrogen Energy, 46 (2021) 20338-20358.
[9] Z. Fan, W. Weng, J. Zhou, D. Gu, W. Xiao, Catalytic decomposition of methane to produce hydrogen: A review, Journal of Energy Chemistry, 58 (2021) 415-430.
[10] R. Siriwardane, J. Riley, C. Atallah, M. Bobek, Investigation of methane and ethane pyrolysis with highly active and durable iron-alumina catalyst to produce hydrogen and valuable nano carbons: Continuous fluidized bed tests and reaction rate analysis, International Journal of Hydrogen Energy, 48 (2023) 14210-14225.
[11] E. Mahmoodzade, F. Meshkani, M. Rezaei, A. Rastegarpanah, Preparation and improvement of nickel catalyst supported ordered mesoporous spherical silica for thermocatalytic decomposition of methane, Journal of the Energy Institute, 93 (2020) 2488-2496.
[12] E. Tezel, H.E. Figen, S.Z. Baykara, Hydrogen production by methane decomposition using bimetallic Ni–Fe catalysts, International Journal of Hydrogen Energy, 44 (2019) 9930-9940.
[13] Y. Wang, Y. Zhang, S. Zhao, J. Zhu, L. Jin, H. Hu, Preparation of bimetallic catalysts Ni-Co and Ni-Fe supported on activated carbon for methane decomposition, Carbon Resources Conversion, 3 (2020) 190-197.
[14] W. Wang, H. Wang, Y. Yang, S. Jiang, Ni–SiO2 and Ni–Fe–SiO2 catalysts for methane decomposition to prepare hydrogen and carbon filaments, International Journal of Hydrogen Energy, 37 (2012) 9058-9066.
[15] P.D. Muley, Y. Wang, J. Hu, D. Shekhawat, Microwave-assisted heterogeneous catalysis, Catalysis: Volume 33, The Royal Society of Chemistry2021, pp. 1-37.
[16] C. Ellison, V. Abdelsayed, M. Smith, D. Shekhawat, Comparative evaluation of microwave and conventional gasification of different coal types: Experimental reaction studies, Fuel, 321 (2022) 124055.
[17] H. Goyal, T.-Y. Chen, W. Chen, D.G. Vlachos, A review of microwave-assisted process intensified multiphase reactors, Chemical Engineering Journal, 430 (2022) 133183.
[18] V. Abdelsayed, C.R. Ellison, A. Trubetskaya, M.W. Smith, D. Shekhawat, Effect of Microwave and Thermal Co-pyrolysis of Low-Rank Coal and Pine Wood on Product Distributions and Char Structure, Energy & fuels., (2019).
[19] U.S.D.o. Energy, Hydrogen Shot, 2021.
[20] C. Jiang, I.W. Wang, X. Bai, S. Balyan, B. Robinson, J. Hu, W. Li, A. Deibel, X. Liu, F. Li, L.M. Neal, J. Dou, Y. Jiang, R. Dagle, J.A. Lopez-Ruiz, G. Skoptsov, Methane Catalytic Pyrolysis by Microwave and Thermal Heating over Carbon Nanotube-Supported Catalysts: Productivity, Kinetics, and Energy Efficiency, Industrial & Engineering Chemistry Research, 61 (2022) 5080-5092.
[21] T. Christiansen, B. Robinson, A. Caiola, C. Jiang, J. Hu, Improved Efficiency of the Microwave-Enhanced Catalytic Pyrolysis of Methane through Supplemental Thermal Heating, Industrial & Engineering Chemistry Research, 61 (2022) 15832-15841.
[22] M. Dadsetan, M.F. Khan, M. Salakhi, E.R. Bobicki, M.J. Thomson, CO2-free hydrogen production via microwave-driven methane pyrolysis, International Journal of Hydrogen Energy, 48 (2023) 14565-14576.

[23] R.R. Mishra, A.K. Sharma, Microwave–material interaction phenomena: Heating mechanisms, challenges and opportunities in material processing, Composites Part A: Applied Science and Manufacturing, 81 (2016) 78-97.
[24] T. Ano, S. Tsubaki, S. Fujii, Y. Wada, Designing Local Microwave Heating of Metal Nanoparticles/Metal Oxide Substrate Composites, The Journal of Physical Chemistry C, 125 (2021) 23720-23728.
[25] C. Bao, A. Serrano-Lotina, M. Niu, R. Portela, Y. Li, K.H. Lim, P. Liu, W.-j. Wang, M.A. Bañares, Q. Wang, Microwave-associated chemistry in environmental catalysis for air pollution remediation: A review, Chemical Engineering Journal, 466 (2023) 142902.
[26] Y. Deng, X. Bai, V. Abdelsayed, D. Shekhawat, P.D. Muley, S. Karpe, C. Mevawala, D. Bhattacharyya, B. Robinson, A. Caiola, J.B. Powell, A.P. van Bavel, J. Hu, G. Veser, Microwave-assisted conversion of methane over H-(Fe)-ZSM-5: Evidence for formation of hot metal sites, Chemical Engineering Journal, 420 (2021) 129670.
[27] F. Zhang, X. Zhang, Z. Song, X. Li, X. Zhao, J. Sun, Y. Mao, X. Wang, W. Wang, Promotion of microwave discharge over carbon catalysts for CO2 reforming of CH4 to syngas, Fuel, 331 (2023) 125914.
[28] W. Deng, Y. Su, S. Liu, H. Shen, Microwave-assisted methane decomposition over pyrolysis residue of sewage sludge for hydrogen production, International Journal of Hydrogen Energy, 39 (2014) 9169-9179.
[29] S. Gadkari, B. Fidalgo, S. Gu, Numerical analysis of microwave assisted thermocatalytic decomposition of methane, International Journal of Hydrogen Energy, 42 (2017) 4061-4068.
[30] B. Fidalgo, L. Zubizarreta, J.M. Bermúdez, A. Arenillas, J.A. Menéndez, Synthesis of carbon-supported nickel catalysts for the dry reforming of CH4, Fuel Processing Technology, 91 (2010) 765-769.
[31] L. Jin, H. Si, J. Zhang, P. Lin, Z. Hu, B. Qiu, H. Hu, Preparation of activated carbon supported Fe–Al2O3 catalyst and its application for hydrogen production by catalytic methane decomposition, International Journal of Hydrogen Energy, 38 (2013) 10373-10380.
[32] J.R.A. Sietsma, A. Jos van Dillen, P.E. de Jongh, K.P. de Jong, Application of ordered mesoporous materials as model supports to study catalyst preparation by impregnation and drying, in: E.M. Gaigneaux, M. Devillers, D.E. De Vos, S. Hermans, P.A. Jacobs, J.A. Martens, P. Ruiz (Eds.) Studies in Surface Science and Catalysis, Elsevier2006, pp. 95-102.
[33] L. Wang, D. Li, M. Koike, S. Koso, Y. Nakagawa, Y. Xu, K. Tomishige, Catalytic performance and characterization of Ni-Fe catalysts for the steam reforming of tar from biomass pyrolysis to synthesis gas, Applied Catalysis A: General, 392 (2011) 248-255.
[34] C. Wildfire, V. Abdelsayed, D. Shekhawat, M.J. Spencer, Ambient pressure synthesis of ammonia using a microwave reactor, Catalysis Communications, 115 (2018) 64-67.
[35] R. Cheng, L. Sun, F. Xu, Y. Luo, C. Zhang, Y. Xia, S. Wei, Y. Guan, M. Zhao, Q. Lin, H. Li, NiFe2O4-Coated Activated Carbon Composite as a Cathode Material for Lithium–Sulfur Batteries, International Journal of Electrochemical Science, 15 (2020) 2624-2633.
[36] K.L. Saenger, J.C. Tsang, A.A. Bol, J. Chu, A. Grill, C. Lavoie, In situ X-ray Diffraction Study of Graphitic Carbon Formed During Heating and Cooling of Amorphous-C/Ni bilayers, Applied Physics Letters, 96 (2010) 153105.
[37] T. Fang-Chang, S. Chi-Min, T. Lung-Chang, M. Ning, W. Yi, W. Sheng, Y. Ying-Kui, Z. Wei, X. Han-Wen, S. Yao-Chi, J. Tao, Carbon Nanotube Industrial Applications, in: M. Jose Mauricio (Ed.) Carbon Nanotubes, IntechOpen, Rijeka, 2011, pp. Ch. 17.